

Hydration Mechanisms and Swelling Behavior of Na-Magadiite

Céline Eypert-Blaison,^{*,†} Emmanuel Sauzéat,[†] Manuel Pelletier,[†]
Laurent J. Michot,[†] Frédéric Villieras,[†] and Bernard Humbert[‡]

Laboratoire Environnement et Minéralurgie, INPL-ENSG-CNRS UMR 7569, BP 40,
54501 Vandoeuvre Cedex, France, and Laboratoire de Chimie Physique Pour l'Environnement,
UMR CNRS-UHP, Nancy I 7564, France

Received July 12, 2000. Revised Manuscript Received November 30, 2000

The hydration behavior of synthetic Na-magadiite was studied by combining thermal analyses, water adsorption gravimetry, X-ray diffraction, and infrared spectroscopy under controlled water pressure. Thermal analyses reveal, at least, two distinct water populations. The water adsorption isotherm exhibits two steps at low relative pressure. These steps correspond to three well-defined interlayer distances on the X-ray diffractograms. Infrared spectra recorded under various water pressures show distinct water populations. For relative pressures ≥ 0.20 , some water molecules (1665 cm^{-1}) are doubly hydrogen bonded, likely to surface sites, whereas other (1625 cm^{-1}) exhibit a signal similar to that observed for hydrated clay minerals at low relative pressures, suggesting a strong influence of the interlayer cation. For lower relative pressures, a single water population at 1635 cm^{-1} is observed, suggesting a dual influence of both the interlayer cation and the surface sites.

Introduction

The hydrous sodium silicates minerals family includes four members: kanemite,¹ makatite,^{2–3} magadiite,⁴ and kenyaite,⁵ which are easily synthesized by hydrothermal reaction of aqueous sodium hydroxide with silica at various $\text{SiO}_2/\text{Na}_2\text{O}$ molar ratios. Reaction composition, reaction temperature, and reaction time determine the final product.

The minerals magadiite and kenyaite were first found in the deposits of Lake Magadi, Kenya, and described by Eugster in 1967.⁴

The chemical composition of natural magadiite was reported as $\text{Na}_2\text{Si}_{14}\text{O}_{29}\cdot 9\text{H}_2\text{O}$.⁴ McAtee *et al.*⁶ and Brindley⁷ showed that its spacing, indexed as d_{001} , changes with water content and that sodium ions are exchangeable. They concluded that magadiite has a layered structure with negatively charged silicate layers compensated by interlayer sodium ions. They also noted the capability of stepwise reversible hydration.

This mineral exhibits a broad range of properties, such as sorption of interlamellar water and polar organic molecules,⁸ cation exchange of interlayer sodium cations,⁹ intracrystalline swelling, grafting, and trans-

formation into crystalline layered silicic acids by proton exchange.¹⁰ Those specific properties promote their application as adsorbents,^{11–12} catalysts supports, cation exchangers, or molecular sieves.¹³

The crystal structure of magadiite remains unknown as no suitable single crystal has ever been obtained. However many structural studies, based on spectroscopic techniques (NMR, IR, Raman, etc.) have been carried out. Three main structures have been proposed:

(i) six-member rings of silica tetrahedra with two inverted tetrahedra per ring;¹⁴

(ii) a combination of five-membered rings as found in some zeolites;¹⁵

(iii) a combination of six- and five-membered rings, and chains of silica tetrahedra.¹⁶

Most studies focus on the solid layer and do not extensively examine the role of interlayer water molecules.

In this paper, we describe the first results obtained on Na-magadiite hydration, studied by a combination of thermal analyses, adsorption experiments, and XRD and IR measurements. Such an approach revealing the structural changes occurring upon water adsorption could also shed new light into the pillaring chemistry of this material. Indeed various studies^{8,13,17–19} have

* Corresponding author.

[†] Laboratoire Environnement et Minéralurgie.

[‡] Laboratoire de Chimie Physique pour l'Environnement.

(1) Johan, Z.; Maglione, J. F. *Bull. Soc. Fr. Minéral. Cristallogr.* **1972**, *95*, 371.

(2) Sheppard, R. A.; Gude, A. J. *Am. Miner.* **1970**, *55*, 359.

(3) Annehed, H.; Fälth, L.; Lincoln, F. J. *Z. Kristallogr.* **1982**, *159*, 203.

(4) Eugster, H. P. *Science* **1967**, *157*, 1177.

(5) Beneke, K.; Lagaly, G. *Am. Miner.* **1983**, *68*, 818.

(6) McAtee, J. L.; House, R.; Eugster, H. P. *Am. Miner.* **1968**, *53*, 2061.

(7) Brindley, G. W. *Am. Miner.* **1969**, *54*, 1583.

(8) Lagaly, G.; Beneke, K.; Weiss, A. *Am. Miner.* **1975**, *60*, 650.

(9) Fletcher, R. A.; Bibby, D. M. *Clays Clay Miner.* **1987**, *35*, 318.

(10) Lagaly, G.; Beneke, K.; Weiss, A. *Am. Miner.* **1975**, *60*, 642.

(11) Kim, C. S.; Yates, D. M.; Heaney, P. J. *Clays Clay Miner.* **1997**, *45*, 881.

(12) Jeong, S. Y.; Lee, J. M. *Bull. Kor. Chem. Soc.* **1998**, *19*, 218.

(13) Wong, S. T.; Cheng, S. *Chem. Mater.* **1993**, *5*, 770.

(14) Pinnavaia, T. J.; Johnson, I. D.; Lipsicas, M. *J. Solid State Chem.* **1986**, *63*, 118.

(15) Garcès, J. M.; Rocke, S. C.; Crowder, C. E.; Hasha, D. L. *Clays Clay Miner.* **1988**, *36*, 409.

(16) Huang, Y.; Jiang, Z.; Schwieger, W. *Chem. Mater.* **1999**, *11*, 1210.

shown that, in contrast with what is observed for other charged layered structures such as swelling clay minerals, pillared magadiite cannot be obtained by direct exchange with bulky polycations in aqueous suspensions. This could be due to the high structural charge of magadiite and/or to different hydration properties preventing a complete delamination of the structure in water.

Experimental Section

Materials. Na-magadiite was synthesized following the procedure described by Fletcher et al.⁹ A mixture of silica (Ludox) and hydrous sodium hydroxide with a molar ratio $\text{SiO}_2:\text{NaOH}:\text{H}_2\text{O} = 9:3:162$, was heated at 150 °C during 42 h under hydrothermal conditions. The final product was leached using NaOH 0.1 mol/L, and dried in air at 70 °C during 12 h.

Methods. Thermal Analysis. Thermogravimetric Analysis (TGA) and Differential Thermal Analysis (DTA) curves were obtained with a Uginé-Eyraud B70 thermobalance Setaram under static air conditions. The weight loss is measured by magnetic compensation. Temperature and DTA signal are measured with Pt–Pt thermocouples, placed under crucibles. The DTA reference is a talc and chlorite mixture, calcined at 1100 °C. The mass of sample is about 100 mg. The results were obtained using a heating rate of 2 °C/min, from 30 °C to 1020 °C.

Controlled-Transformation-Rate Thermal Analysis (CTR-TA), described by Rouquerol,²⁰ is coupled with a quadrupole mass spectrometer. In this process, the heating rate is not fixed, but directly depends on the gas pressure generated by outgassing or reactions occurring during sample heating. The experimental conditions selected in the present study were a sample mass of 235 mg, a residual pressure of 2 Pa, and a heating rate of 1 °C/min, from –196 to 400 °C. Between –196 °C and 20 °C, the increase in temperature is not controlled by pressure and corresponds to the free heating of the sample at a rate of ≈ 0.5 °C/min. From 20 °C upward, true CTRTA conditions are used with a maximal heating rate of 2 °C/min. The apparatus is coupled with a mass spectrometer to identify and quantify gas emission. The mass spectra were obtained on a Balzers QMG 420C mass spectrometer.

Adsorption Experiments. Nitrogen adsorption–desorption isotherms at –196 °C were obtained using a lab-built classical step by step volumetric setup. Prior to the experiments, the samples were outgassed at 50 °C under a residual pressure of 0.1 Pa during 18 h. Surface area was determined using the BET treatment.

Water vapor gravimetric adsorption experiments were carried out using a lab built quasi-equilibrium setup designed around a Setaram MTB 10-8 symmetrical microbalance. Water vapor was supplied to the sample (thermostated at 30 °C) from a source kept at 41 °C, at a slow flow rate to ensure quasi-equilibrium conditions at all times. The simultaneous recording of mass uptake and equilibrium pressure directly yields the water vapor adsorption isotherm. The experimental conditions were a sample mass of 105 mg and an outgassing at 50 °C during 18 h under a residual pressure of 1 Pa.

The evolution of X-ray diffraction patterns with water relative pressure was followed using a specially designed experimental setup. The oriented sample was placed inside a chamber allowing the control of relative humidity and temperature. The chamber kept at 30 °C is connected to a water vapor source. The water relative pressure in the chamber is controlled by changing the temperature of the source. X-ray diffraction patterns are recorded simultaneously over 30° (θ) on an Inel CPS 120 curved detector using transmission

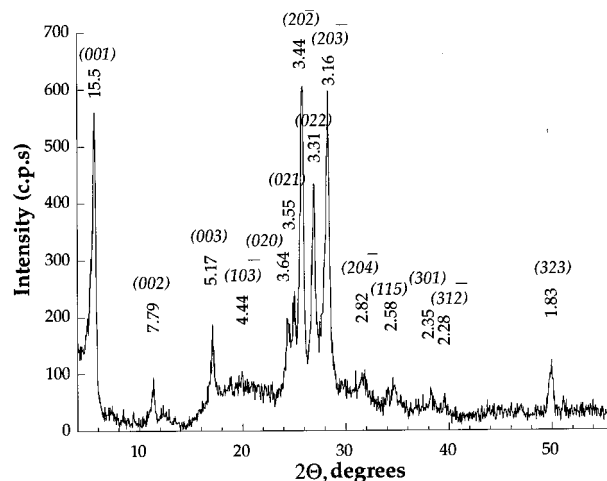


Figure 1. X-ray powder diffraction data of synthesized Na-magadiite.

geometry with Co K α radiation. The sample is outgassed before experiment at 50 °C under a residual pressure of 10^{-3} Torr during 24 h. For each hydration state, the X-ray diffraction patterns were recorded after 24 h equilibrium time.

The evolution of infrared spectra with water relative pressure was investigated in-situ, using a special lab-built infrared transmission cell.²¹ The temperature and moisture of the sample are controlled. The chamber is connected to a water vapor source, and the water relative pressure in the chamber is controlled by changing its temperature between –20 and +26.2 °C \pm 0.1 °C. In these experiments, the deposit obtained after drying a 5 g/L suspension of magadiite on a ZnSe plate, was kept at 30 °C \pm 0.1 °C. Under such conditions, the relative water vapor pressure in the cell ranges between 0.006 and 0.85. The cell is equipped with ZnSe windows in order to widen the IR range investigated. The FT-IR spectra were recorded on a Bruker IFS-55 FT-IR spectrometer, using a DTGS detector. The IR transmission spectra consisted of 100 averaged scans in the range 7000–400 cm^{-1} , with a resolution of 2 cm^{-1} . The spectra were recorded at least 24 h after changing the temperature of the water vapor source.

Results and Discussion

X-ray diffraction patterns (Figure 1) and chemical analyses reveal the single phase Na-magadiite character of the synthesized sample, in agreement with JCPDS 42-1350.

According to chemical analyses results, the unit cell formula of magadiite can be written as $\text{Na}_2\text{Si}_{13.5}\text{O}_{28} \cdot 8.9\text{H}_2\text{O}$. Such a formula is classical for synthesized magadiite. Garcès et al.¹⁵ compared literature data on compositions of natural and synthetic magadiites samples: the $\text{SiO}_2/\text{Na}_2\text{O}$ mole ratios range from about 12 to about 14, and the water content ranges from about 8 to 18 wt %. The differences in water content were attributed to differences in drying used by several authors, and the differences in $\text{SiO}_2/\text{Na}_2\text{O}$ mole ratios were assigned to impurities and various synthesis conditions employed.

Thermal Analysis. Figure 2 presents the thermogravimetric analysis of the magadiite sample. The TGA curve exhibits a 15.2% weight loss, between 30 and 1000 °C. The main weight loss below 200 °C (13%) can be

(17) Sprung, R.; Davis, M. E.; Kauffman, J. S.; Dybowski, C. *Ind. Eng. Chem. Res.* **1990**, *29*, 213.

(18) Dailey, J. S.; Pinavaia, T. J. *Chem. Mater.* **1992**, *4*, 855.

(19) Döring, J.; Beneke, K.; Lagaly, G. *Colloid Polym. Sci.* **1992**, *270*, 609.

(20) Rouquerol, J. *J. Therm. Anal.* **1970**, *2*, 123.

(21) Pelletier, M.; de Donato, P.; Thomas, F.; Michot, L. J.; Gérard, G.; Cases, J. M. In *Clays for our future*, Proceedings of the 11th International Clay Conference; Kodama, H., Mermut, A. R., Torrance, J. K., Eds.; Ottawa, Canada, 1997; p 555.

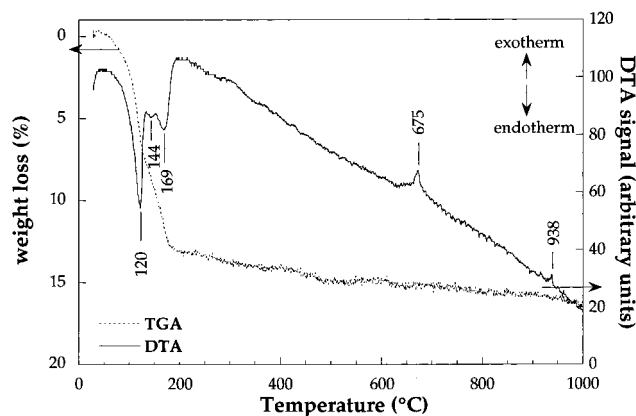


Figure 2. Conventional thermogravimetric analysis of Na-magadiite: TGA and DTA curves.

assigned to dehydration. Above 200 °C, little mass loss occurs ($\approx 2\%$), which is assigned to silanol condensation into siloxanes. Lagaly and co-workers¹⁰ showed that the dehydrated form is stable up to 500 °C and can be fully rehydrated, which proves that no structural changes, affecting the solid layer, occurs before 500 °C.

Above 200 °C, the DTA curve shows two exothermic peaks at 675 and 938 °C, attributed to quartz and trydimite crystallization, respectively.

Below 200 °C, three endothermic peaks are observed at 120, 144, and 169 °C on the DTA curve. Similar features were reported by Lagaly et al.¹⁰ and Brandt et al.²² Lagaly et al.,¹⁰ using a temperature ramp of 10 °C/min, observed two broad endothermic peaks around 180 and 230 °C, whereas Brandt et al.²² using a temperature ramp of 3 °C/min, observed two main peaks at 115 and 170 °C, with a unmentioned intermediate small peak at 145 °C.

All these results suggest, at least, two steps in dehydration, i.e., two different hydration states in magadiite.

As shown in the case of fibrous clay minerals^{23,24} or smectites,^{25–26} CTRTA is a very appropriate technique for investigating the various types of hydration water molecules. However, in the case of samples with weakly bound solvation water, the use of vacuum techniques starting at room temperature, such as CTRTA, can result in some information loss. Such difficulty can be circumvented by starting the analyses at much lower temperature, e.g., liquid nitrogen temperature.

Figure 3 represents the derivative curve of the weight loss, calculated from the intensity of the mass 18, analyzed by mass spectroscopy. The corresponding weight loss, 13%, is the same as that obtained by TGA, between 30 and 200 °C.

The derivative curve displays three peaks, at -14 , 15, and 25 °C, which might correspond qualitatively to the different water types observed by DTA. The much lower

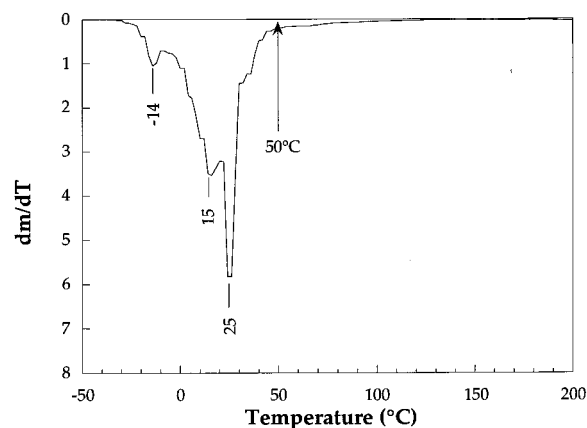


Figure 3. Derivative curve obtained from CTRTA experiment, for mass 18.

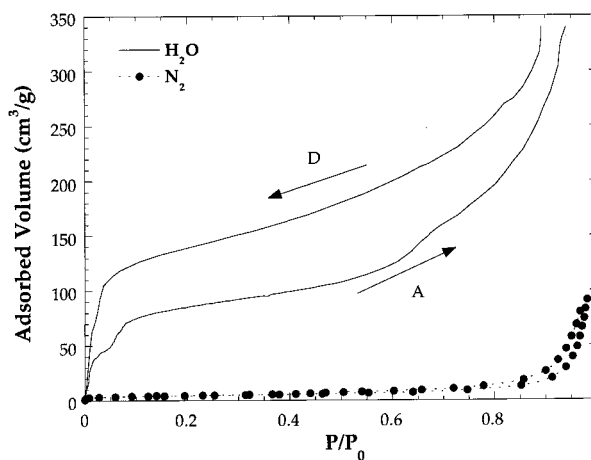


Figure 4. Water vapor adsorption–desorption isotherm at 30 °C, and nitrogen adsorption–desorption isotherm at -196 °C, onto magadiite.

temperature, compared with DTA, reveals the effect of vacuum on magadiite dehydration.

On the basis of an analogy with other lamellar solids with interlayer sodium cations,^{27,28} the three water families observed by all thermal analyses could be tentatively assigned to:

- (i) water close to the liquid state, and probably located in mesopores;
- (ii) physically sorbed water molecules and molecules from the outer hydration sphere of sodium cations;
- (iii) strongly bound water molecules in the inner hydration sphere of sodium cations and hydroxyl groups.

Gas Adsorption Experiments. Isotherm Determination. On the basis of CTRTA experiments, an outgassing temperature of 50 °C was chosen for pretreating the samples before adsorption. Indeed, as shown in Figure 3, at such temperature, under vacuum, all hydration water is evacuated.

The nitrogen adsorption–desorption isotherm is presented in Figure 4. Magadiite appears nearly non-microporous and presents some mesopores that can be assigned to interparticular porosity. The BET specific surface area is $14 \text{ m}^2 \cdot \text{g}^{-1}$.

(22) Brandt, A.; Schwieger, W.; Bergk, K. H.; Grabner, P.; Porsch, M. *Cryst. Res. Technol.* **1989**, *24*, 47.

(23) Grillet, Y.; Cases, J. M.; François, M.; Rouquerol, J.; Poirier, J. E. *Clays Clay Miner.* **1988**, *36*, 233.

(24) Cases, J. M.; Grillet, Y.; François, M.; Michot, L.; Villieras, F.; Yvon, J. *Clays Clay Miner.* **1991**, *39*, 191.

(25) Cases, J. M.; Bérend, I.; Besson, G.; François, M.; Uriot, J. P.; Thomas, F.; Poirier, J. E. *Langmuir* **1991**, *8*, 2730.

(26) Bérend, I.; Cases, J. M.; François, M.; Uriot, J. P.; Michot, L.; Masion, A.; Thomas, F. *Clays Clay Miner.* **1995**, *43*, 324.

(27) Poinsignon, C.; Cases, J. M.; Fripiat, J. J. *J. Phys. Chem.* **1978**, *82*, 1855.

(28) Poinsignon, C.; Yvon, J.; Mercier, R. *Isr. J. Chem.* **1982**, *22*, 253.

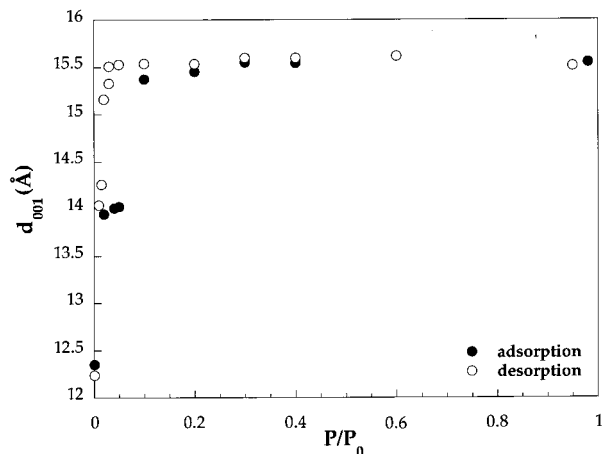


Figure 5. Evolution of the experimental 001 reflection of magadiite with water vapor relative pressure at 30 °C.

In comparison with nitrogen, the amount of water adsorbed is much higher (Figure 4) and yields a BET surface area around $190 \text{ m}^2 \cdot \text{g}^{-1}$, assuming a cross-sectional area of 0.148 nm^2 for adsorbed water molecules.²⁹ This isotherm presents an hysteresis in desorption, which is conserved down to very low relative pressures as the two branches never really merge. The observed differences with nitrogen adsorption and the irregular shapes of both the adsorption (A) and desorption (D) branches suggest complex water adsorption mechanisms. This isotherm is then likely indicative of structural changes occurring upon water adsorption due to the increased availability of the interlamellar region to water molecules. The low pressure evolution is particularly striking as two well-resolved steps are observed in the region before $P/P_0 = 0.1$. The adsorbed amount at the first plateau of the isotherm for $P/P_0 = 0.04$ (3.8%) corresponds to the weight loss observed by TGA between 150 and 180 °C (3.6%). This confirms that at least two distinct hydrated states develop upon adsorption of the “first” water molecules.

Another slope change can be noticed at $P/P_0 \approx 0.7$. This slope change can be tentatively assigned to capillarity condensation in rather calibrated mesopores resulting from the arrangement of magadiite in rosette-like particles.^{15,19,30} This interpretation is confirmed by the nitrogen adsorption isotherm, that presents a small shape change around $P/P_0 = 0.75\text{--}0.80$.

X-ray Diffraction. To probe the structural changes occurring along the water adsorption isotherm, we followed the basal distance $d(001)$ with water relative pressure (Figure 5). Under vacuum at room temperature, the 001 reflection corresponds to a basal spacing of 12.3 Å. Such change in interlamellar distance with vacuum was already observed by Brindley⁷ and Lagaly et al.¹⁰ The evolution upon water adsorption is remarkable as it exhibits two well-defined steps and matches perfectly the water adsorption isotherm for low relative pressure. The basal spacing remains constant for $0.02 < P/P_0 < 0.05$ and increases again sharply to reach a value of 15.3 Å at $P/P_0 = 0.1$. The basal spacing then increases slowly to 15.5 Å at $P/P_0 = 0.3$ and remains

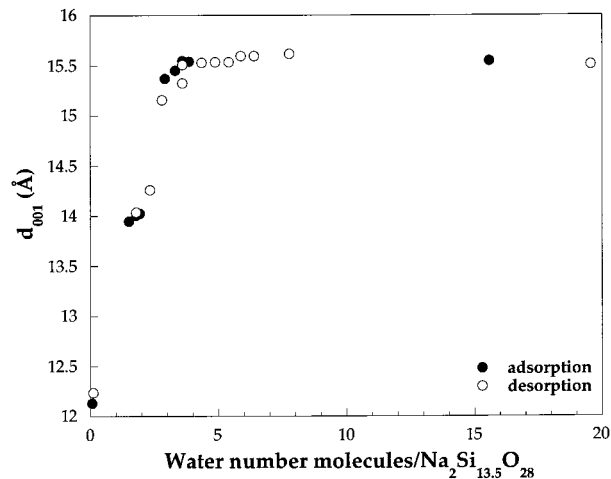


Figure 6. Number of water molecules per unit cell versus basal distance, during adsorption and desorption of water vapor onto magadiite.

constant thereafter. The swelling appears to be limited to a maximum value of 15.5 Å which suggests that layer stacks with an interlayer distance around 15 Å could be present in aqueous suspensions of Na-magadiite. In desorption, the basal spacing has a constant value of 15.5 Å down to $P/P_0 = 0.04$ and then sharply decreases to 12.3 Å without any marked step around 14 Å.

Such evolution of $d_{(001)}$ shows unambiguously that the first water molecules adsorb in the interlayer of Na-magadiite, provoking an expansion of the structure along the c -axis. The values of d spacing obtained on the two steps cannot be assigned to the development of simple water layers as observed in swelling clay minerals, where both experiments and simulation^{31,32} reveal a $d_{(001)}$ increase by steps of 3 Å.

The step observed on the water adsorption isotherm (Figure 4) for $P/P_0 \approx 0.7$ does not correspond to any increase in d spacing. This somewhat confirms the previous assignment of this feature to condensation in mesopores.

Valuable information on the structural evolution of magadiite upon water adsorption can be obtained by combining water adsorption and XRD results to plot the evolution of d spacing as a function of the number of adsorbed water molecules by unit cell (Figure 6). Such plot reveals that adsorption and desorption curves are superimposed, which shows that water uptake and release are governed by the same mechanisms. The hysteresis observed in the water adsorption isotherm must then be related to different activation energies. Furthermore, it appears that the two swelling steps observed, from 12.3 to 14 Å and from 14 to 15.5 Å, correspond to the adsorption of two and four water molecules per unit cell, respectively.

Infrared Measurements. To investigate in more depth the status and location of water molecules in magadiite, we followed the evolution of infrared spectra with water adsorption. Indeed, as shown in numerous studies dealing with the hydration of swelling clay minerals^{21,27,33,34} infrared spectroscopy can provide de-

(29) Hagymassy, J.; Brunauer, S.; Mikhail, R. S. H. *J. Colloid Interface Sci.* **1969**, *29*, 485.

(30) Kruse, H. H.; Beneke, K.; Lagaly, G. *Colloid Polym Sci.* **1989**, *267*, 844.

(31) Suquet, H.; De la Calle, C.; Pezerat, H. *Clays Clay Miner.* **1975**, *23*, 1.

(32) Ben Brahim, J.; Armagan, N.; Besson, G.; Tchoubar, D. *J. Appl. Crystallogr.* **1983**, *16*, 264.

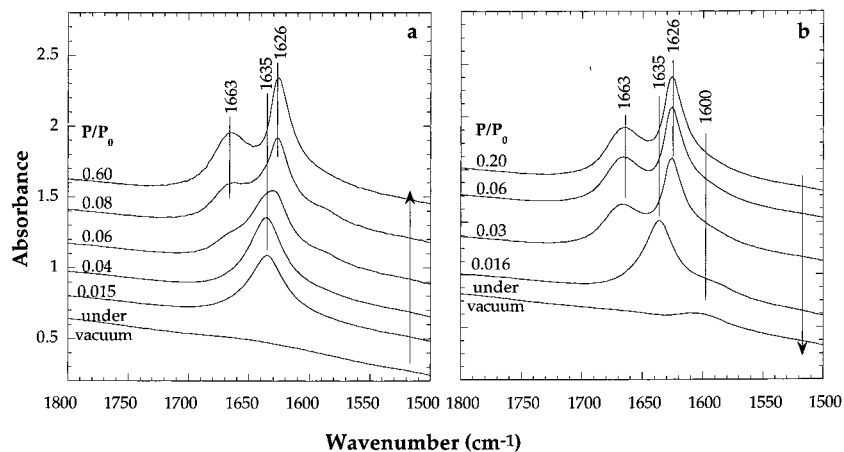


Figure 7. Evolution of infrared spectra (2000–1600 cm⁻¹) of Na-magadiite at 30 °C upon water adsorption (a), and water desorption (b).

tailed information about water structure in interlayer spaces.

The evolution of the bending band (ν_2) of water molecules with increasing water vapor relative pressure is presented in Figure 7a for selected relative pressure values.

When the sample is put under vacuum, it appears nearly fully dehydrated as the water deformation band is barely visible. For a relative pressure of 0.015, i.e., in the first step of opening of the interlayer space, a single bending band is observed at 1635 cm⁻¹. For a relative pressure of 0.06, i.e., in the second opening step, the maximum of the ν_2 band shifts toward lower wavenumbers at 1626 cm⁻¹ and a shoulder appears at 1665 cm⁻¹. The shape of the bending band also suggests that the 1635 cm⁻¹ component is still present. Indeed, a decomposition of the $\delta_{\text{H}_2\text{O}}$ region was performed, and the results confirm the presence of at least three components around 1665, 1635, and 1626 cm⁻¹. For higher relative pressures, the three populations are still present, and two distinct maxima are observed at 1626 and 1663 cm⁻¹. The evolution in desorption is strictly parallel, which confirms the reversibility of hydration phenomena. The only difference observed between adsorption and desorption lies in the presence of a residual component around 1600 cm⁻¹ after completion of an adsorption–desorption cycle. This signal seems to be related to an organic pollution from the pumping system and does not then bear any real significance. Indeed, some tests performed on the empty IR cell after long periods under static vacuum revealed the presence of organic molecules with a similar IR signature on the ZnSe windows. The 1635 cm⁻¹ position is similar to that observed for liquid water.³⁵ The position at 1626 cm⁻¹ is typical of water molecules interacting with Na⁺ cations as observed in swelling clay minerals^{34,36} whereas the position at 1663 cm⁻¹ characterizes doubly hydrogen bonded water molecules. Such doublet in the region 1670–1620 cm⁻¹ was also observed by Rojo et al.³⁷ and

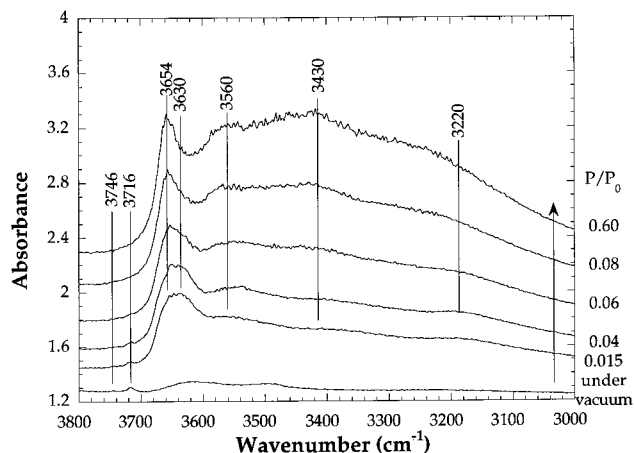


Figure 8. Evolution of the infrared spectra (4000–3000 cm⁻¹) of Na-magadiite at 30 °C upon water adsorption.

Huang et al.¹⁶ and was attributed to either the existence of several crystallographically nonequivalent water molecules in the unit cell or the correlation splitting of ν_2 . The single band at 1635 cm⁻¹, observed for very low relative pressure, has never been described. With regard to the structural changes occurring at low relative pressure, it seems difficult to interpret the position at 1635 cm⁻¹ as corresponding to liquid water. Another interpretation could be to relate the position of this band to what is observed in some binary water/organic bases 1:1 complexes, where $\delta \text{H}_2\text{O}$ around 1634 cm⁻¹ can be obtained.³⁴ In our case, this would mean that the first water molecule are in a C_1 symmetry with two non-equivalent OH vibrations. In such case, this should be observed in the OH stretching region by the simultaneous appearance of both low- and high-frequency signals.

Figure 8 presents the evolution of IR spectra with water relative pressure in the OH stretching region.

Under vacuum, one can observe two small bands at 3746 and 3716 cm⁻¹, assigned to SiOH groups with very little hydrogen bonding,³⁹ and two broad bands at about

(33) Prost, R. *Ann. Agron.* **1975**, *26*, 463.

(34) Sposito, G.; Prost, R. *Chem. Rev.* **1982**, *82*, 553.

(35) Franck, H. S. In *Water. A Comprehensive Treatise*; Francks, F., Eds.; Plenum Press: New York, 1972.

(36) Johnston, C. T.; Sposito, G.; Erickson, C. *Clays Clay Miner.* **1992**, *40*, 722.

(37) Rojo, J. M.; Ruiz-Hitzky, E.; Sanz, J. *J. Inorg. Chem.* **1988**, *27*, 2785.

(38) Bricknell, B. C.; Ford, T. A.; Letcher, T. M. *Spectrochim. Acta* **1997**, *53A*, 299.

(39) Legrand, A. P.; Hommel, H.; Tuel, A.; Vidal, A.; Balard, H.; Papirer, E.; Levitz, P.; Czernichowski, M.; Erre, R.; Van Damme, H.; Gallas, J. P.; Hemidy, J. F.; Lavalley, J. C.; Barrès, O.; Burneau, A.; Grillet, Y. *Adv. Colloid Interface Sci.* **1990**, *33*, 91.

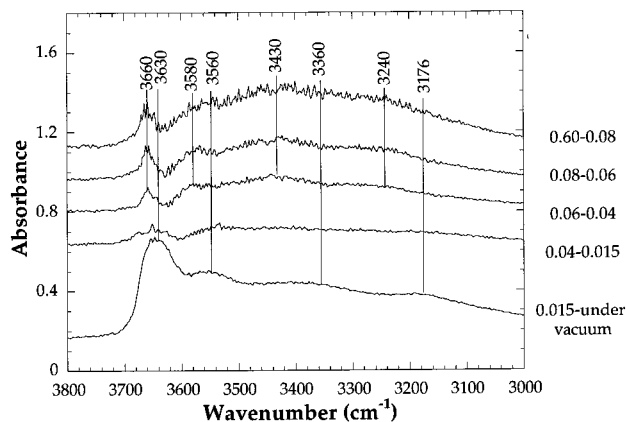


Figure 9. Spectrum to spectrum subtraction of infrared signals in the range (4000–3000 cm^{-1}) for Na-magadiite conditioned under various water vapor relative pressure.

3615 and 3490 cm^{-1} , that could correspond to remaining hydration water. This apparent contradiction with what was observed in the bending region (no visible hydration signal in Figure 7a) is certainly due to differences in absorption coefficient for the bending and stretching components of water molecules,⁴⁰ the stretching region being far more sensitive than the bending one. Upon hydration, changes are noticeable in both the high-frequency range (3800–3600 cm^{-1}) and low-frequency range (<3600 cm^{-1}). To better evidence such changes, subsequent spectra were subtracted from each other (Figure 9).

Between vacuum and $P/P_0 = 0.015$, new signals appear at 3630, 3560, 3360, and 3176 cm^{-1} . If one considers the evolution of absorption coefficients with frequency,³⁹ the signals at 3360 and 3176 cm^{-1} are overestimated with regard to their true relative abundance. Therefore, the very first adsorption step is mainly linked to the appearance of two bands at 3630 and 3560 cm^{-1} . Such positions confirm the assignment of the 1635 cm^{-1} component to water molecules in C_1 symmetry, as such a wavenumber triplet can be observed in 1:1 complexes between water and organic bases, such as for instance C_4H_8O .³⁸ The intensity and width of the 3630 cm^{-1} component suggests that some water molecules are also involved in the creation of SiOH groups. For $0.015 < P/P_0 < 0.04$, in agreement with water adsorption isotherm, XRD measurements, and IR spectra in the OH bending region, only very limited changes occur. In all this relative pressure range, the initial components at 3716 and 3746 cm^{-1} do not seem to be affected by water adsorption (no negative peaks in the subtraction). Such behavior is in agreement with the low reactivity of isolated and geminal silanol groups toward water, observed for silica.³⁹

For $0.04 < P/P_0 < 0.06$, new components at 3660, 3580, 3430, and 3240 cm^{-1} appear. This clearly reveals a second hydration stage. As classically observed in studies dealing with hydration, an univocal assignment of the various signals in the stretching region is a rather difficult task. Still, the pattern observed is coherent with the assignments deduced from the IR study in the bending region, i.e., water molecules interacting with sodium cations and doubly hydrogen bonded water

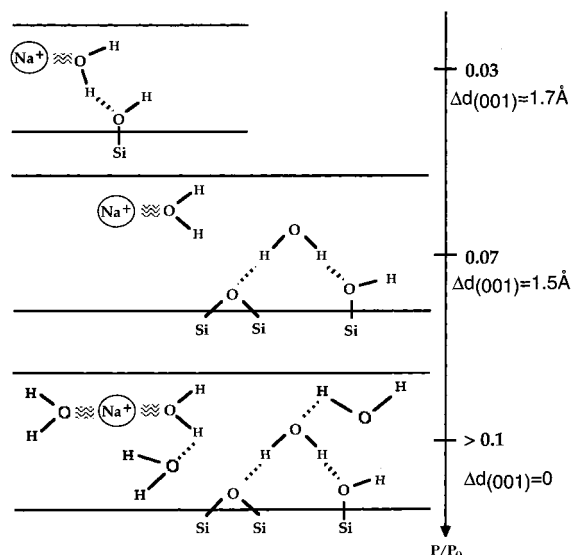


Figure 10. Idealized scheme for the different hydration steps of Na-magadiite.

molecules. For $P/P_0 > 0.06$, the four components keep on growing. As far as relative intensities are concerned, the 3430 cm^{-1} component is affected the most, which suggests that at high relative pressure, adsorbed water molecules are mainly in a strongly hydrogen bonded state.

Conclusion

The combination of thermal analyses, water adsorption gravimetry, and spectroscopic techniques (XRD, IR) appears as a very powerful tool to study water adsorption mechanisms in swelling minerals. Using such an approach, we can propose the following scheme (Figure 10) for describing water adsorption in Na-magadiite in three main steps.

In a first hydration step, for $0 < P/P_0 < 0.05$, water molecules adsorb mainly in the interlayer space of Na-magadiite. This first hydration stage is clearly evidenced by a step in the water adsorption isotherm corresponding to the uptake of two water molecules per unit cell, i.e., one water molecule per Na^+ cation. Such uptake provokes a 1.7 Å expansion of the interlamellar distance. The exact structure and location of water molecules remains uncertain, as part of these water molecules may be engaged in the creation of silanol groups. Still, the major part interact simultaneously with both the surface and sodium cations, as revealed by infrared experiments.

The second hydration stage, for $0.05 < P/P_0 < 0.10$, also mainly involves the interlayer space and corresponds to the adsorption of a second water molecule per Na^+ cation, as observed on the water adsorption isotherm. It is associated with a further d spacing increase of 1.5 Å and the growth of two infrared bands at 1626 and 1663 cm^{-1} . These bands reveal two distinct water populations: the first one interacts mainly with the Na^+ cation and is relatively free of hydrogen bonding, whereas the second one is doubly hydrogen bonded. The evolution of the infrared spectra in this range suggests that the structural changes, in this second stage, involve some kind of reorganization of the water molecules observed in the first hydration stage.

(40) Carteret, C. Thesis, Université Henri Poincaré Nancy, 1999.

For higher relative pressures, up to $P/P_0 \approx 0.7$, the uptake of water molecules is rather monotonic and does not provoke any further structural change. Spectroscopic data suggest that, in this stage, the adsorption of water molecules is predominantly due to the filling of empty spaces in the interlayer region. The infrared signals observed still reveal water molecules with free OH groups, which proves that a true liquid water structure does not develop in the interlayer region.

The swelling pathway evidenced for Na-magadiite is markedly distinct from what is observed in other swelling minerals, such as smectites or vermiculites, where $\approx 3 \text{ \AA}$ swelling steps are usually observed. Furthermore, the structure of interlayer hydration

water appears very different. Cation hydration alone does not explain water adsorption in this mineral as surface chemistry also plays a major role in structuring water molecules. The relative importance of surface and cation contribution should be solved by combining (i) additional structural studies of Na-magadiite and (ii) a study of the hydration behavior for magadiite exchanged with various cations.

Acknowledgment. We acknowledge Dr. Sabine Petit (CNRS-UMR 6532, Poitiers) for providing us with the synthetic Na-magadiite sample used in this study.

CM001130+